Applied Catalysis A: General 383 (2010) 102–111

Contents lists available at ScienceDirect

Applied Catalysis A: General

journal homepage: www.elsevier.com/locate/apcata

Effects of NaOH solution treatment on the catalytic performances of MCM-49 in liquid alkylation of benzene with ethylene

Kefeng Liu [a,b], Sujuan Xie [a], Guoliang Xu [a], Yuning Li [a], Shenglin Liu [a], Longya Xu [a,*]

[a] State Key Laboratory of Catalysis, Dalian Institute of Chemical Physics, Chinese Academy of Sciences,Dalian 116023, PR China
[b] Graduate University of Chinese Academy of Science, Beijing 100049, PR China

ARTICLE INFO

Article history:
Received 20 November 2009
Received in revised form 10 May 2010
Accepted 20 May 2010
Available online 27 May 2010

Keywords:
MCM-49
Alkali-treatment
Benzene
Ethylene
Liquid alkylation

ABSTRACT

MCM-49 zeolite was alkali-treated with NaOH solutions under mild and severe conditions. The samples before and after alkali-treatment were both used as catalysts in liquid alkylation reaction of benzene with ethylene. XRD, XRF, TPD, TPO, IR, SEM, ^{29}Si NMR, N_2 adsorption and desorption techniques were employed to characterize the samples. The mildly alkali-treated samples exhibited higher catalytic stability than the parent HMCM-49, as the amorphous particles on the MCM-49 crystal surface were cleaned and the diffusion of the reactant and product was enhanced. The severe alkali-treatment condition resulted in the selective extraction of silicon atoms and the introduction of extra mesopores. The catalytic stability of the catalysts that had been severely alkali-treated was not as good as that of mildly treated ones, but was still better than that of the parent HMCM-49 catalyst if the alkali-treatment conditions were not too severe.

1. Introduction

Ethylbenzene is an important raw material in the petrochemical industry [1]. At present, most ethylbenzene is used as feedstock for the production of styrene [2,3], an important material for plastic and rubber production. Nowadays, more than 90% of ethylbenzene is produced by the alkylation of benzene with ethylene catalyzed by acidic substances. The conventional catalyst for this process is $AlCl_3$, which still accounts for 24% of the worldwide ethylbenzene production in 2009. As utilization of this catalyst involves problems of separation, handling, safety and corrosion [4], immense efforts have been devoted to the development of new catalysts for ethylbenzene production.

Compared with $AlCl_3$, zeolites possess advantages in easy separation, low corrosion, high surface area as well as uniform microporous structure coupled to shape selectivity, and thus they are better acidic catalysts when applied in petrochemical industry [5]. When zeolites are used as catalyst, there are mainly two kinds of processes: vapor-phase and liquid-phase processes. Compared with the vapor-phase process, liquid-phase process exhibits obvious advantages such as better thermal control, higher selectivity to target products and longer catalyst life [4]. Zeolites such as USY, Beta and MCM-22 have been used as catalysts in the liquid-phase alkylation processes [1,3,4,6]. Although MCM-22 catalyst is somewhat low in catalytic activity, it exhibits higher selectivity for ethylbenzene. Interestingly, it was reported that MCM-49, which possesses a structure nearly identical to that of the calcined MCM-22 [7–9], showed even higher ethylbenzene selectivity than MCM-22 [10].

Although MCM-49 exhibits good catalytic performances in some petrochemical processes, the small sizes of its apertures and cavity channel greatly limit the diffusion of reactants and products with large molecules [5,11]. An effective way to reduce diffusion limitation is to introduce mesopores into zeolites by post-treatment. Steam treatment and acid leaching are useful methods to produce irregular mesopores by removing aluminium from zeolites, but at the same time the acid properties of such samples are seriously affected [12–14]. Different from the methods above, works of Groen et al. [15,16], Tao et al. [11,17] and our group [18] indicate that alkali-treatment is also an effective way to introduce mesopores into most zeolites.

Additionally, many zeolites, especially those abundantly synthesized and post-treated in factories, contain amorphous silico-aluminate. And these particles may hinder the diffusion of molecules into/out of pores when zeolites are used as catalysts or adsorbents. Subjecting zeolites to a caustic solution can remove these amorphous materials, which can result in the improvement of diffusion and catalytic properties [19–22].

In this study, hierarchically structured MCM-49 samples were prepared through a controlled silicon extraction by severe alkali-

* Corresponding author at: Dalian Institute of Chemical Physics, Chinese Academy of Sciences, 804 Group, #457 Zhongshan Road, Dalian 116023, Liaoning, PR China. Tel.: +86 411 84693292; fax: +86 411 84693292.
E-mail address: lyxu@dicp.ac.cn (L. Xu).

0926-860X/$ – see front matter © 2010 Elsevier B.V. All rights reserved.
doi:10.1016/j.apcata.2010.05.029

Table 1
Alkali-treatment conditions and chemical compositions of MCM-49 before and after alkali-treatment.

Catalysts	c_{NaOH} (mol/l)	Temperature (°C)	Time (min)	Si/Al_2[a] (mol ratio)
HMCM-49	–	–	–	20.4
0.1AT–75C–120M	0.10	75	120	20.1
0.2AT–75C–120M	0.20	75	120	17.0
0.5AT–75C–120M	0.50	75	120	15.0
0.65AT–75C–120M	0.65	75	120	13.5
0.8AT–75C–120M	0.80	75	120	11.9
0.1AT–25C–30M	0.10	25	30	20.7
0.1AT–75C–30M	0.10	75	30	20.4
0.025AT–25C–3M	0.025	25	3	20.8
0.025AT–25C–15M	0.025	25	15	20.9
0.025AT–25C–30M	0.025	25	30	21.0
0.025AT–25C–60M	0.025	25	60	21.8

[a] Measured by XRF.

treatment, and the MCM-49 zeolite catalysts with high crystallinity were prepared by mild alkali-treatment. The parent and alkali-treated HMCM-49 samples were both applied for the liquid-phase alkylation reaction of benzene with ethylene. The catalytic performances of the catalysts were well correlated to their porous structures and acidic properties.

2. Experimental

2.1. Catalyst preparation

The calcined MCM-49 zeolite (Si/Al_2 molar ratio = 20.4) was provided by Tieling catalyst factory of China. The as-received MCM-49 was treated with NaOH solutions (m (zeolite):V (solution) = 1:10 (g/ml)) with certain concentrations at two different temperatures (25 and 75 °C) under vigorously stirring for various times. Then the mixture was cooled down by ice water and the solid was recovered by filtrating, washing and drying. Subsequently, the as-received MCM-49 or the treated samples were ammonium exchanged in 0.8N NH_4NO_3 solution at 75 °C for three times, and the final H-form zeolite was obtained by calcination of the NH_4-form zeolite at 540 °C for 4 h. Before evaluation, all the samples were pelletized, crushed and sieved to 20–40 mesh particles.

The alkali-treatment conditions and the chemical compositions of the prepared samples are listed in Table 1. The sample without alkali-treatment was named as HMCM-49, while the alkali-treated samples were named as xAT–yC–zM, where x, y and z represent NaOH concentration (N), treatment temperature (°C) and time (min), respectively. For example, 0.1AT–75C–120M is an MCM-49 sample which was alkali-treated in 0.1N NaOH solutions at 75 °C for 120 min.

2.2. Characterizations

X-ray diffraction (XRD) patterns of samples were obtained on an X Pert Pro X-ray diffractometer operated at 40 kV and 40 mA using Cu Kα radiation. The relative crystallinity of the samples was calculated according to the sum of the peak intensities at 2θ of 10.0°, 14.3°, 16.0°, 22.7° and 26.0°.

The chemical composition of MCM-49 samples was analyzed on a Philips Magix 601X X-ray fluorescence (XRF) spectrometer.

The morphology of the samples was investigated by scanning electron microscopy (SEM) on an FEI Quanta-200F field emission scanning electron microscope.

^{29}Si NMR experiments were carried out on a Bruker DRX-400 spectrometer using 4 mm ZrO_2 rotors. The spectra were recorded at 79.5 MHz with the magic angle-spinning rate of 4 kHz.

N_2 adsorption and desorption measurements were carried out at −196 °C on an ASAP 2010 instrument. Prior to analysis, the samples were pretreated at 350 °C in the vacuum of 10^{-3} Pa for 5 h.

NH_3 temperature programmed desorption (NH_3-TPD) was used for the measurement of acid distribution. In a typical run, 0.1400 g of sample was loaded in a U-shaped quartz micro-reactor (i.d. = 4 mm) connected to an on-line gas chromatograph (Shimadzu GC-8A) equipped with a TCD detector. Before the NH_3-TPD measurement, the catalyst was pretreated at 600 °C for 1 h in flowing He (25 ml/min), then cooled down to 150 °C and saturated with NH_3. After a flat baseline was obtained, TPD process was carried out from 150 to 600 °C at a heating rate of 18.8 °C/min.

Infrared (IR) measurements were performed on a Bruker 70 IR spectrometer. For the framework IR detection, samples were mixed with KBr (m_{sample}:m_{KBr} = 1:100), and the mixtures were pressed into wafers with a diameter of 13 mm. The spectrum of a KBr wafer of the same size was used as background. For the pyridine adsorption IR (Py-IR), the sample was first pressed into a self-supported wafer and then the wafer was pretreated at 500 °C for 2 h in vacuum (10^{-2} Pa). After cooling down to the room temperature, a spectrum was recorded as background. Subsequently, the wafer was exposed to the pyridine vapor for 20 min at 0 °C, and then outgassed at 150 °C for 30 min. IR spectra were collected at room temperature. The Brønsted/Lewis acid (B/L) molar ratio was calculated according to the determination methods reported in Ref. [23].

Temperature program oxidations (TPO) of used catalysts were carried out in a U-shaped quartz micro-reactor (i.d. = 4 mm) connected to an on-line mass spectrometer (MS). In a typical run, 0.0800 g of used sample was loaded in the reactor and heated from 50 to 850 °C at a heating rate of 10 °C/min with the flowing of 10% O_2/Ar (50 ml/min).

2.3. Catalyst evaluation

The liquid alkylation of benzene with ethylene was carried out in a stainless-steel fixed bed reactor. In a typical run, 2 g of catalyst was located in the center of the reactor and pretreated at 500 °C for 1 h in nitrogen. After the reactor was cooled down to 220 °C, benzene was pumped into the reactor to fully fill the bed before ethylene was introduced. The reaction conditions, which ensured that the reaction was performed in liquid-phase, were as follows: 3.5 MPa of pressure, 220 °C of temperature, 0.5 and 1.5 h^{-1} of weight hourly space velocity (WHSV) of ethylene, 12/1 of benzene/ethylene molar ratio. The product was analyzed by Varian 3800 gas chromatograph with a flame ionization detector (FID).

3. Results

3.1. Severe alkali-treatment of MCM-49 zeolite

In the following experiments, MCM-49 is severely alkali-treated in 0.1–0.8N NaOH solution for 120 min at 75 °C. From the chemical compositions of the parent and treated samples listed in Table 1, it

can be observed that the Si/Al_2 molar ratio of 0.1AT–75C–120M is similar to that of HMCM-49, while it decreases from 20.4 to 11.9 with increasing the NaOH solution concentration from 0.2 to 0.8N. The results suggest that Si is more easily extracted from framework than Al, which is consistent with the results in Refs. [11,24].

Table 2 presents the textural properties of the samples. With the increase of NaOH solution concentration from 0.1 to 0.65N, the mesopore volume of the samples increases from 0.29 to 0.40 cm^3/g and the extra surface area (S_{ext}) increases from 79.2 to 174.2 m^2/g. In contrast, the microporous area decreases from 409.1 to 241.2 m^2/g.

XRD patterns and relative crystallinity of the samples are shown in Fig. 1(A). The diffraction pattern of HMCM-49 is in agreement with that in Ref. [8]. Compared with HMCM-49 (relative crystallinity: 100%), the relative crystallinity of 0.1AT–75C–120M increases to 134%, which may be attributed to the purification of zeolite by cleaning the amorphous particles [20]. With increasing the NaOH solution concentration from 0.2 to 0.65N, the relative crystallinity of samples decreases from 86 to 40%. Especially, as the NaOH solution concentration is 0.8N, only 9% of relative crystallinity is left.

^{29}Si NMR spectra are employed to investigate the chemical environment of the framework silicon atoms in MCM-49. The deconvoluted spectra show that there are at least five resonance peaks that can be attributed to different chemical environments of T sites (where T is tetrahedral site in the proposed hexagonal structure of MCM-49) in Q^4 region (Fig. 2). Some of these peaks are overlapped due to the similar chemical shifts [25,26]. The resonance peak at about −106 ppm is usually attributed to Si (0Al) on T2 site, although some contribution from Si (1Al) site cannot be excluded. The peak at −121(−116) ppm (marked as $T1^+$ ($T6^+$)) is mainly ascribed to Si on T1 (T6) site, and it may also contain some contribution from silicon atoms on T4 and T5 sites [27,28]. It is clear that some of the peak intensity decreases upon alkali-treatment severity (through increasing NaOH solution concentration). In particular, the peaks at −121 ($T1^+$) and −114.5 ppm (T3) shrink more obviously than the others (T2, T7 and T8), along with the increase of peak area at about −98 ppm of Q3 (Fig. 2(B)). The deconvolution quantification data of $T1^+$ and $Q3^+$ (some contribution of Q2 possibly involved) for several samples are calculated and listed in Table 3.

In Fig. 3, the framework IR spectra of the samples are depicted. The vibrations at about 1080, 800 and 450 cm^{-1} are assigned to the "internal" structure vibrations of the SiO_4 or AlO_4 tetrahedra. The absorption bands between 540 and 630 cm^{-1} are related to the presence of double rings in the framework [29,30]. From the deconvoluted spectra in Fig. 3(B), we can see that the peak intensity of blocks (550 cm^{-1}) and 5MR chains (1250 cm^{-1}) decreases with the increase of NaOH solution concentration, especially when it is higher than 0.2N, indicating the partial damage of the 5MR structures after the severe alkali-treatment.

Fig. 4 displays the SEM images of the parent and alkali-treated samples. The sample HMCM-49 (Fig. 4(a)) exhibits morphology of 5–30 μm aggregates constituted of thin crystal sheets 30–40 nm of thick. Apertures between the sheets of HMCM-49 are stacked with very small particles (Fig. 4(a)) which are absent in the as-received NaMCM-49. This might be due to the instability of MWW type zeolite while it is calcined in air [29,31,32]. After being alkali-treated with 0.1N NaOH solution, the sheets of sample are maintained and the small particles between the sheets disappear (Fig. 4(b)). The outer surface of the crystal sheet starts to dissolve when the NaOH solution concentration increases to 0.2N, as is marked out in Fig. 4(c). When the concentration amounts to 0.5N, most sheets on the surface of the aggregates are destroyed. When the concentration is increased to 0.65N, even the aggregates collapse and only cracked sheets are left as shown in Fig. 4(e), due to the quite serious alkali-treatment [33].

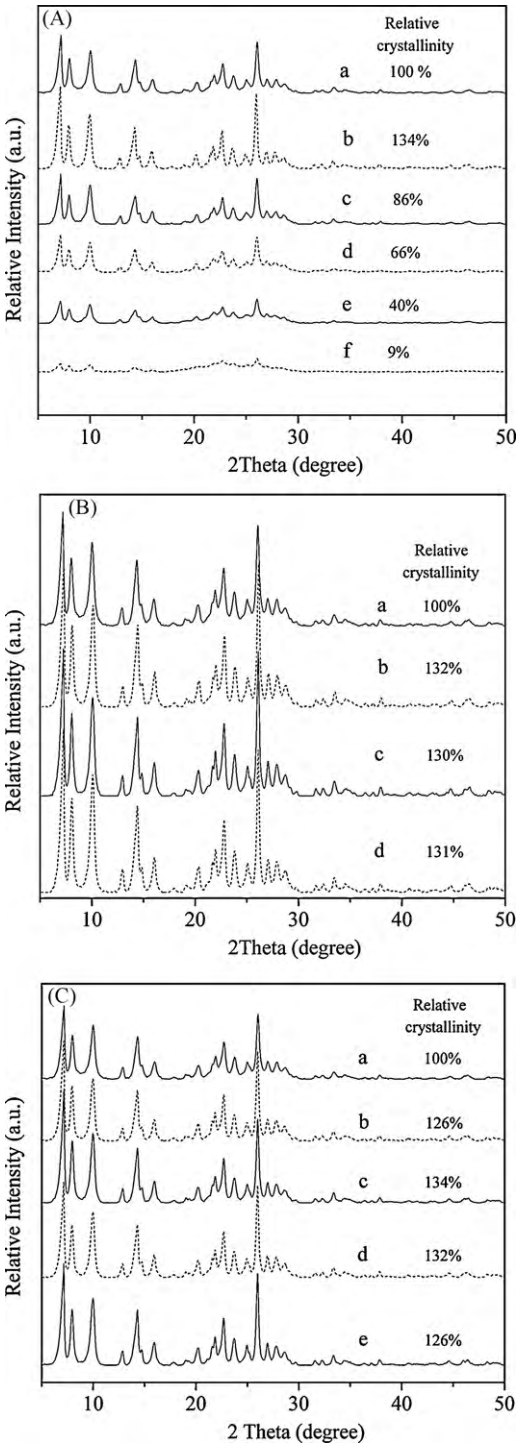

Fig. 1. XRD patterns of samples before and after alkali-treatment. (A) a: HMCM-49, b: 0.1AT–75C–120M, c: 0.2AT–75C–120M, d: 0.5AT–75C–120M, e: 0.65AT–75C–120M and f: 0.8AT–75C–120M; (B) a: HMCM-49, b: 0.025AT–25C–30M, c: 0.1AT–25C–30M and d: 0.1AT–75C–30M; (C) a: HMCM-49, b: 0.025AT–25C–3M, c: 0.025AT–25C–15M, d: 0.025AT–25C–30M and e: 0.025AT–25C–60M.

The acidity of HMCM-49 samples before and after alkali-treatment was characterized by the NH_3-TPD method (Fig. 5). The quantitative results shown in Fig. 5 and Table 3 were obtained according to Gauss curve fitting by peak deconvolution method. The experimental curves are satisfactorily fitted by at least three peaks

Table 2
Texture properties of samples before and after alkali-treatment.

Catalysts	S_{BET} (m^2/g)	S_{micro} (m^2/g)	S_{ext} (m^2/g)	V_{micro} (cm^3/g)	V_{meso} (cm^3/g)
HMCM-49	488.3	409.1	79.2	0.20	0.29
0.1AT–75C–120M	458.4	368.1	90.3	0.18	0.29
0.2AT–75C–120M	469.1	354.2	114.9	0.17	0.30
0.5AT–75C–120M	461.3	301.4	159.9	0.15	0.38
0.65AT–75C–120M	415.4	241.2	174.2	0.11	0.40
0.1AT–25C–30M	448.0	372.2	75.8	0.18	0.26
0.1AT–75C–30M	437.2	378.1	59.2	0.19	0.19
0.025AT–25C–3M	489.0	407.6	81.4	0.20	0.30
0.025AT–25C–15M	442.7	385.2	57.5	0.19	0.24
0.025AT–25C–30M	431.9	378.6	53.3	0.19	0.21
0.025AT–25C–60M	402.3	361.0	41.3	0.18	0.19

Table 3
Acid properties and deconvoluted Si NMR results of samples before and after alkali-treatment.

Catalysts	*B*/*L*	Acid quantity (mmol/g)			$T1^+$ (%)	$Q3^+$(%)
		Weak	Medium	Strong		
HMCM-49	1.97	0.16	0.19	0.44	11.52	8.28
0.1AT–75C–120M	1.87	0.19	0.19	0.49	11.49	8.25
0.2AT–75C–120M	1.67	0.26	0.15	0.40	8.66	8.95
0.5AT–75C–120M	1.46	0.32	0.13	0.35	4.17	9.60
0.65AT–75C–120M	1.32	0.35	0.10	0.29	1.33	11.22

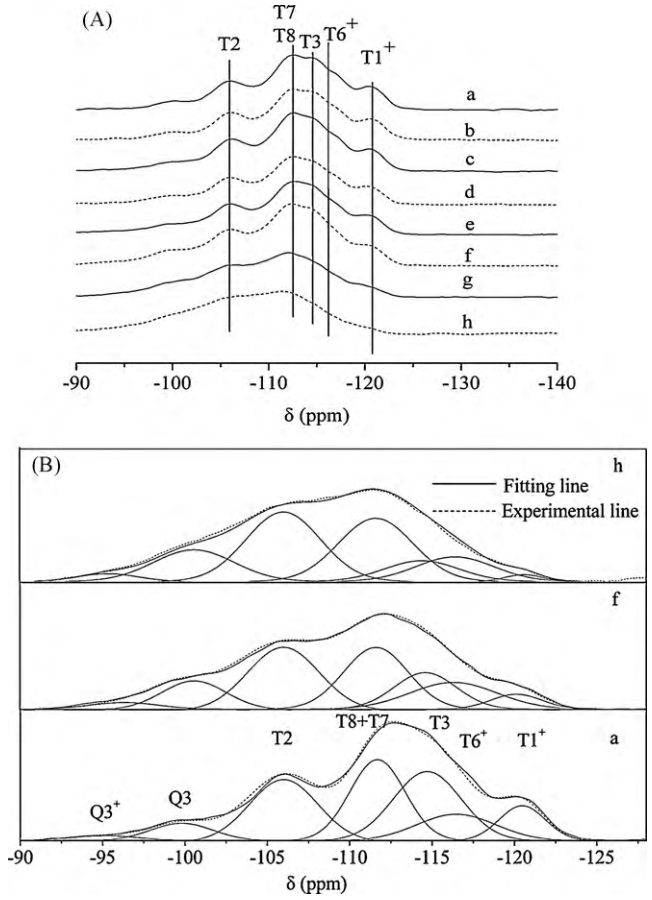

Fig. 2. (A) ^{29}Si NMR spectra of MCM-49 zeolite catalysts before and after alkali-treatment: a: HMCM-49, b: 0.025AT–25C–3M, c: 0.025AT–25C–15M, d: 0.025AT–25C–30M, e: 0.1AT–75C–120M, f: 0.2AT–75C–120M, g: 0.5AT–75C–120M and h: 0.65AT–75C–120M. (B) Deconvoluted ^{29}Si NMR spectra of a: HMCM-49, f: 0.2AT–75C–120M and h: 0.65AT–75C–120M. $T1^+$ ($T6^+$): peak at −121(−116) ppm mainly included Si on T1 (T6) site, may also involve Si on T4 or T5 site. $Q3^+$: peak at about −98 ppm is mainly contributed by Q3 type Si, Q2 type Si may be also partly included ($Q_n = Si(OSi)_n(OH)_{(4-n)}$).

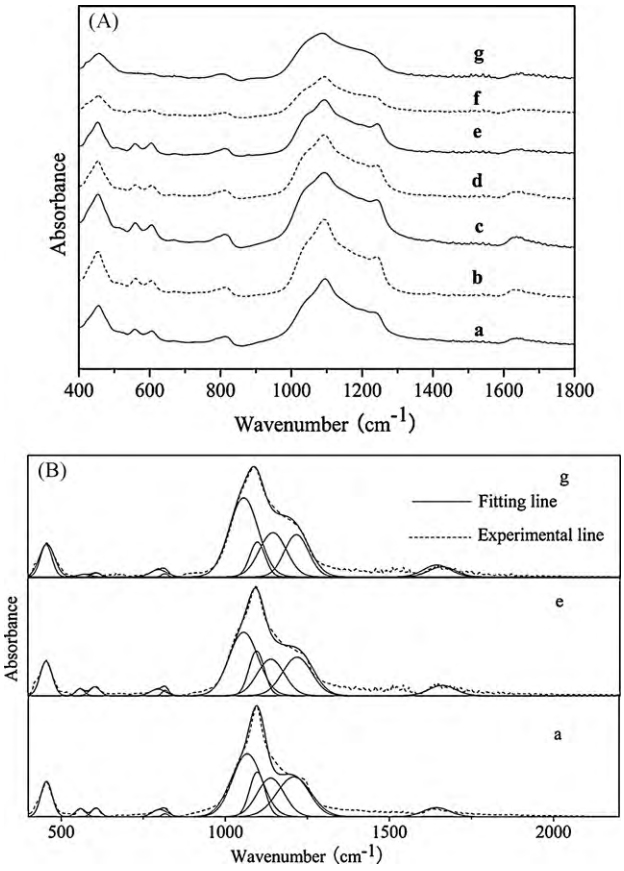

Fig. 3. (A) Framework IR spectra of samples before and after alkali-treatment: a: HMCM-49, b: 0.025AT–25C–3M, c: 0.025AT–25C–15M, d: 0.025AT–25C–30M, e: 0.2AT–75C–120M, f: 0.5AT–75C–120M and g: 0.65AT–75C–120M. (B) Deconvoluted Framework IR spectra of a: HMCM-49, e: 0.2AT–75C–120M and g: 0.65AT–75C–120M.

that represent three types of acid sites with different strengths (Fig. 5A(e)). These three peaks centered at about 246, 317 and 430 °C are denoted as weak, medium and strong acid sites, respectively. For the samples alkali-treated under severe conditions, each

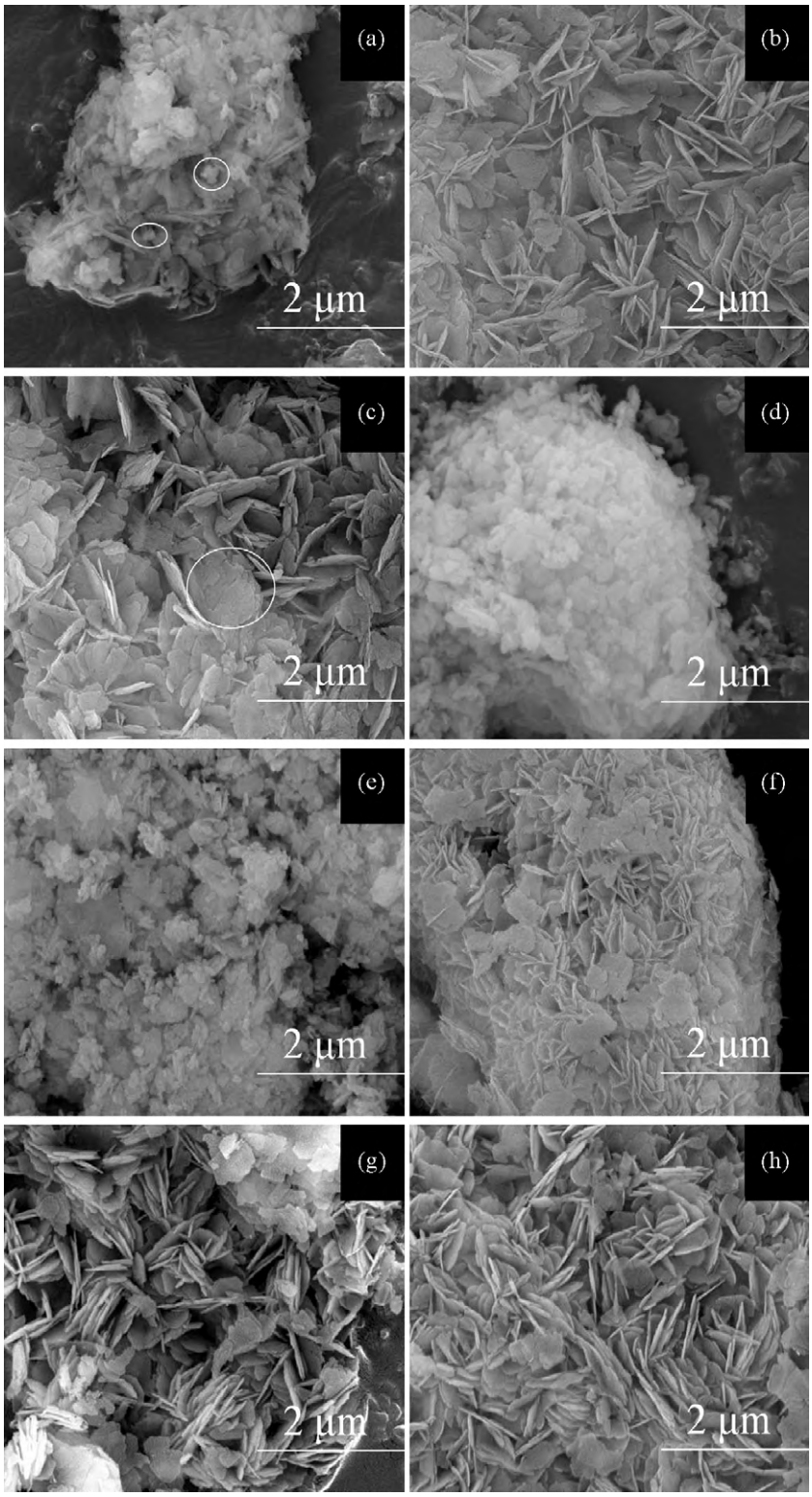

Fig. 4. SEM of MCM-49 zeolite catalysts before and after alkali-treatment. (a): HMCM-49, (b) 0.1AT–75C–120M, (c) 0.2AT–75C–120M, (d) 0.5AT–75C–120M, (e) 0.65AT–75C–120M, (f) 0.025AT–25C–15M, (g) 0.025AT–25C–30M and (h) 0.025AT–25C–60M.

total acid amount is all around 0.80 mmol/g. However, the medium and strong acid amounts as well as the *B*/*L* ratio decrease obviously when the NaOH solution concentration increases from 0.1 to 0.65N (Table 3), which means that the medium and strong acid sites and the Brønsted acid sites are more sensitive to caustic solution than are the weak acid sites and the Lewis acid sites.

3.2. Mild alkali-treatment

The results in Section 3.1 indicate that mesopores can be produced in the MCM-49 zeolite when the NaOH concentration of alkali-treatment is higher than 0.2N. However, the crystallinity of MCM-49 zeolite cannot be preserved, which is dissimilar to the situation in the case of ZSM-5 [18,34]. Further investigations are

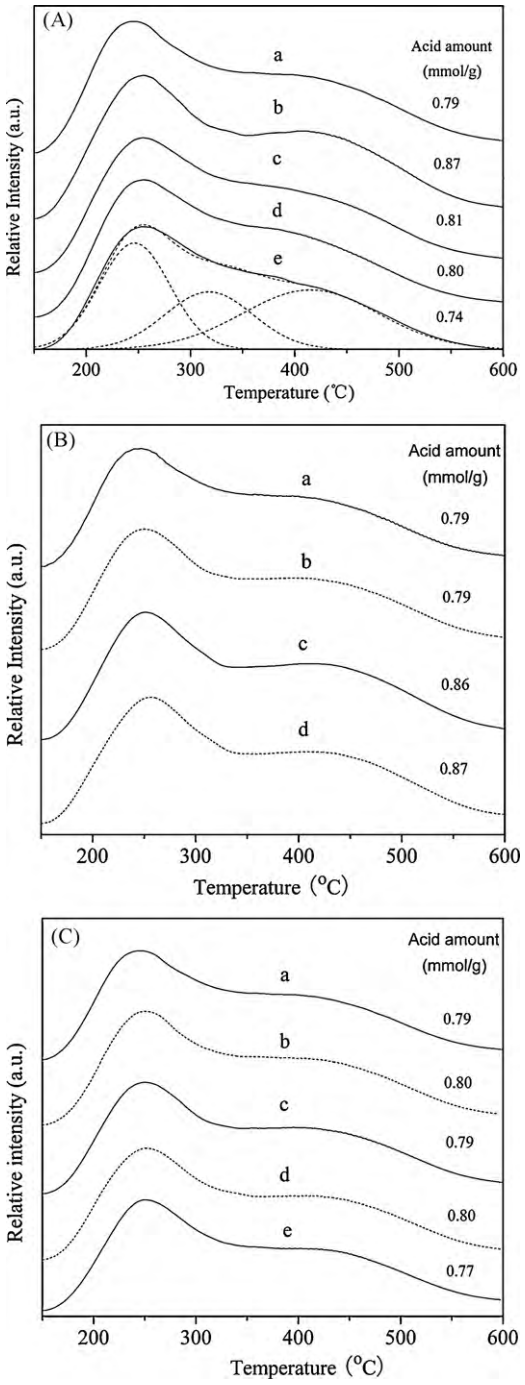

Fig. 5. NH_3-TPD spectra of MCM-49 zeolites catalysts before and after alkali-treatment. (A) a: HMCM-49, b: 0.1AT–75C–120M, c: 0.2AT–75C–120M, d: 0.5AT–75C–120M and e: 0.65AT–75C–120M. (B) a: HMCM-49, b: 0.025AT–25C–30M, c: 0.1AT–25C–30M and d: 0.1AT–75C–30M. (C) a: HMCM-49, b: 0.025AT–25C–3M, c: 0.025AT–25C–15M, d: 0.025AT–25C–30M and e: 0.025AT–25C–60M.

carried out under mild alkali-treatment conditions, during which the crystallinity of the samples can be well preserved or even increased, as shown in Table 1 and Fig. 1.

The influences of the NaOH solution concentration and treatment temperature on mild alkali-treated MCM-49 zeolite are firstly investigated by preparing the samples of 0.025AT–25C–30M, 0.1AT–25C–30M and 0.1AT–75C–30M. The effect of alkali-treatment time is also studied by immersing MCM-49 zeolite in the 0.025N NaOH solutions at 25 °C for 3, 15, 30 and 60 min. All the MCM-49 samples alkali-treated under the mild conditions possess high relative crystallinity (~130%, Fig. 1(B and C)) and similar Si/Al_2 molar ratios to that of the parent sample (~20, Table 1). In addition, the total acid amount and the B/L ratio of these samples show little difference (~0.8 mmol/g and ~1.9, respectively). Furthermore, the distribution of their weak, medium and strong acid amount (not be listed here) shows little change compared with that of HMCM-49.

As shown in Table 2, the microporous properties of MCM-49 zeolites are not obviously affected by the alkali-treatment with NaOH solution of 0.025N at 25 °C. Even if the alkali-treatment time is prolonged to 60 min, 90% of microporous area and of volume are preserved. However, the mesoporous related properties are affected intensively. When the treatment time is increased from 0 (HMCM-49) to 60 min, the S_{ext} decreases from 79.2 to 41.3 m^2/g and the V_{meso} decreases from 0.30 to 0.19 cm^3/g. This means that the mesopores formed by the aggregation of small particles [1,35] are reduced by these mild alkali-treatment.

As shown in Fig. 1(C), when MCM-49 is mildly alkali-treated in an NaOH solution of 0.025N for different times, the samples show high and similar relative crystallinity (~130%). The ^{29}Si NMR spectra show that the intensity distributions of the five peaks of 0.025AT–25C–3M, 0.025AT–25C–15M and 0.025AT–25C–30M are quite similar (Figs. 2(A)(b–d)), and the FT-IR spectra (Figs. 3(A)(b–d)) also exhibit similar framework vibrations, indicating that the zeolite frameworks are slightly affected. In addition, as shown in Fig. 4(f–h), similar to 0.1AT–75C–120M, small particles disappear when the samples are treated in NaOH solution of 0.025N. Clear crystal sheets and the aggregates can be observed in the samples of 0.025AT–25C–15M, 0.025AT–25C–30M and 0.025AT–25C–60M, which is different from the case for the samples treated in NaOH solution of ≥0.2N (Fig. 4(c–e)).

3.3. Evaluation of the MCM-49 catalysts

The parent and alkali-treated HMCM-49 samples were both used as catalysts for the liquid alkylation of benzene with ethylene. Ethylene conversion changes with the time on stream (TOS), while the product distributions have little difference. As shown in Table 4, the ethylation selectivity is over 99.0% for all the samples, and the selectivity to toluene is lower than 0.1%.

The evolutions of ethylene conversion with the TOS over the MCM-49 catalysts are shown in Fig. 6. For the parent HMCM-49 and the alkali-treated samples under severe conditions (Fig. 6(A)), their initial ethylene conversions are all at ~99.9%, indicating that the MCM-49 catalysts are very active for this reaction. However, the catalytic stability of the parent HMCM-49 is not very good, ethylene conversion decreases from 99.9% at 1 h of TOS to 91.0% at 27 h. The catalytic stability is improved over the alkali-treated MCM-49 zeolite catalysts except for the severely treated sample of 0.65AT–75C–120M. At TOS of 27 h, the ethylene conversions over the xAT–75C–120M samples where x = 0.1, 0.2 and 0.5 are 97.6%, 94.5% and 93.8%, respectively.

For the samples alkali-treated with 0.1N NaOH solution, the milder the conditions are (by reducing the treatment temperature and treatment time), the better the corresponding catalytic stability is (Fig. 6(A) iconograph). When the concentration of NaOH solution is 0.025N, there is almost no difference for the performances of the catalysts alkaki-treated for different times at the ethylene WHSV of 0.5 h^{-1} (ethylene conversion is always higher than 99.0% within 27 h of TOS). In order to differentiate the catalytic performances, we enhanced the ethylene WHSV to 1.5 h^{-1}. As shown in Fig. 6(B), the catalyst, even alkali-treated for only 3 min at 25 °C in NaOH solution of 0.025N shows higher ethylene conversion and better catalytic stability than HMCM-49. When the treatment time was between 3 and 60 min, the samples show similar initial ethylene conversion, but their catalytic stability varies with the treatment time. Among

Table 4
Reaction performance over the MCM-49 catalysts via alkali-treatment conditions (a) HMCM-49, (b) 0.65AT–75C–120M, (c) 0.5AT–75C–120M, (d) 0.2AT–75C–120M, (e) 0.1AT–75C–30M, (f) 0.025AT–25C–15M and (g) 0.025AT–25C–30M.

Catalysts	a^x	b^x	c^x	d^x	e^x	a^y	e^y	f^y	g^y
Ethylene conversion (mol%)	96.9	82.9	98.4	99.7	99.9	76.0	89.7	92.1	91.4
Product selectivity (mol%)									
Ethyl benzene	95.1	96.2	95.7	96.1	96.2	97.2	96.4	96.6	97.4
m-Diethyl benzene	1.4	1.0	1.5	1.3	1.5	0.8	1.1	1.1	0.7
p-Diethyl benzene	1.2	0.9	1.2	1.1	0.9	0.7	0.9	0.8	0.6
o-Diethyl benzene	1.6	1.5	1.1	1.1	0.9	1.1	1.3	1.2	0.9
$\sum$ (Ethylation)	99.3	99.6	99.5	99.6	99.5	99.8	99.7	99.7	99.6
Methylbenzene	0.07	0.1	0.07	0.08	0.08	0.04	0.03	0.1	0.1
C9 aromatics	0.05	0.03	0.07	0.06	0.03	0.01	0.01	0.02	0
$C10^+$ aromatics	0.56	0.25	0.33	0.23	0.37	0.11	0.23	0.17	0.28
Paraffins	0.02	0.02	0.03	0.03	0.02	0.04	0.03	0.01	0.02

Reaction conditions: 3.5 MPa, 220 °C, 9 h of TOS, *B*/*E* (mol ratio) 12. *x*: 0.5 h^{-1} of ethylene WHSV and *y*: 1.5 h^{-1} of ethylene WHSV.

all these samples investigated, 0.025AT–25C–15M shows the best catalytic performances.

The TPO technique was employed to investigate the nature of coke deposited on the used samples. As shown in Fig. 7, three peaks centered at about 345, 440 and 620 °C can be seen in the TPO curve of HMCM-49. The TPO curves of the mildly alkali-treated samples (x = 0.025 and 0.1N) are very close to that of HMCM-49 (Fig. 7(B and C)), indicating that the total coking amount and carbon species generated in the alkylation reaction are very similar. The TPO peaks shift to lower-temperature positions for the severely alkali-treated samples ($c_{NaOH} \geq$ 0.2N), especially for the peak at ~620 (to 550 °C for 0.65AT–75C–120M). In addition, the intensity of peaks of the severely alkali-treated samples decrease compared with that on HMCM-49.

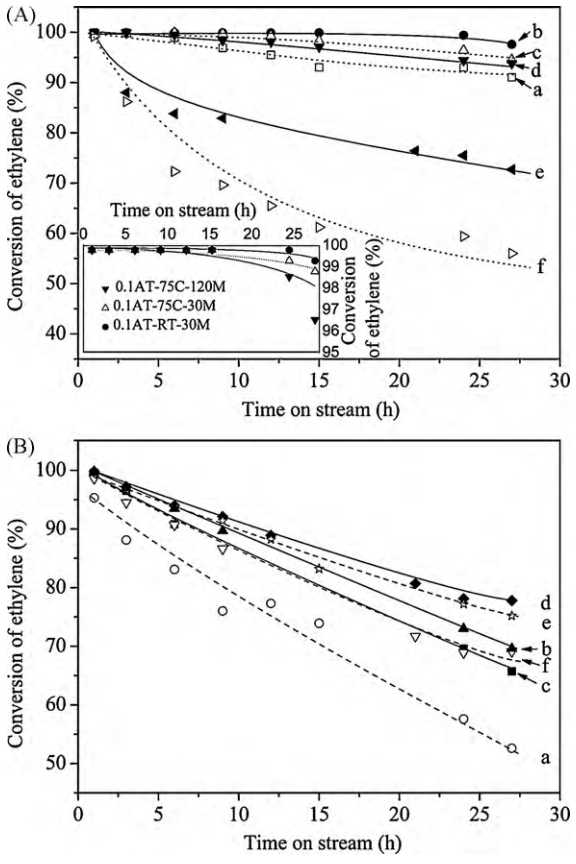

Fig. 6. Ethylene conversion as a function of reaction time over the MCM-49 zeolite catalysts. (A) 3.5 MPa, 220 °C, *B*/*E* (mol ratio) = 12, ethylene WHSV = 0.5 h^{-1}: a: HMCM-49, b: 0.1AT–75C–120M, c: 0.2AT–75C–120M, d: 0.5AT–75C–120M, e: 0.65AT–75C–120M and f: 0.8AT–75C–120M. (B) 3.5 MPa, 220 °C, *B*/*E* (mole ratio) = 12, ethylene WHSV = 1.5 h^{-1}: a: HMCM-49, b: 0.1AT–25C–30M, c: 0.025AT–25C–3M, d: 0.025AT–25C–15M, e: 0.025AT–25C–30M and f: 0.025AT–25C–60M.

4. Discussion

According to the results above, the structure evolutions of the MCM-49 catalysts during the alkali-treatment process can be depicted as in Scheme 1. It is well known that HMCM-49 is composed of crystal sheets with "pockets" (hemi-supercages) on the external surfaces (Scheme 1(A)) [7]. The amorphous particles generated by calcinations may scatter between the sheets and partly fill in the pockets if they are small enough, which results in the hindered diffusion for substance into/out of the "pockets". The aggregation of these small particles produces inter-particle mesopores, which contributes a lot to the mesopore volume and extra surface area [35].

For the MCM-49 samples alkali-treated under the severe conditions, the fact that the relative crystallinity of 0.1AT–75C–120M is higher than that of HMCM-49 (Fig. 1(A)) is mainly attributed to the purification of zeolite [20,22]. Bonilla et al. investigated the effect of alkali-treatment conditions on ferrierite zeolite and found that too severe extraction of Si atoms would lead to collapse of the zeolite framework [36]. Bao and co-workers also showed that the relative crystallinity of ZSM-5 would decrease with the increase of alkali-treatment severity [37,38]. However, unlike ZSM-5, the relative crystallinity of MCM-49 (Si/Al_2 molar ratio = 20.4) cannot be preserved when the concentration of NaOH solution is above 0.2N, and it is only 40% when the concentration of NaOH solution is 0.65N, which indicates that the framework of MCM-49 zeolite is less stable than that of ZSM-5 [18].

When the NaOH solution concentration is higher than 0.2N, the external surface area and mesopore volume of the sample obtained increase along with the loss of micropores (Table 2, Scheme 1(C)). The formation of mesopores can be ascribed to the extraction of Si from framework, during which a little amount of Al is also eluted [39,40]. Bao and co-workers and Groen et al. investigated the alkali-treated MFI type zeolite by N_2 adsorption and reported that the extraction of Si usually started from the boundaries and defects [37,41]. On the alkali-treated ZSM-5, Ogura et al. found that the dissolution of Si started from the surface of zeolite crystals [42]. In our experiments, the morphology of MCM-49 changes with the severe alkali-treatment conditions. For the severely alkali-treated MCM-49 samples (Fig. 4(c–e)), the edges of crystal sheets, especially sheets on the surface of aggregates, are dissolved. According to the Ref. [37], the boundaries and defects are the places where the crystallization is poor, and they are easily dissolved in the alkali solution.

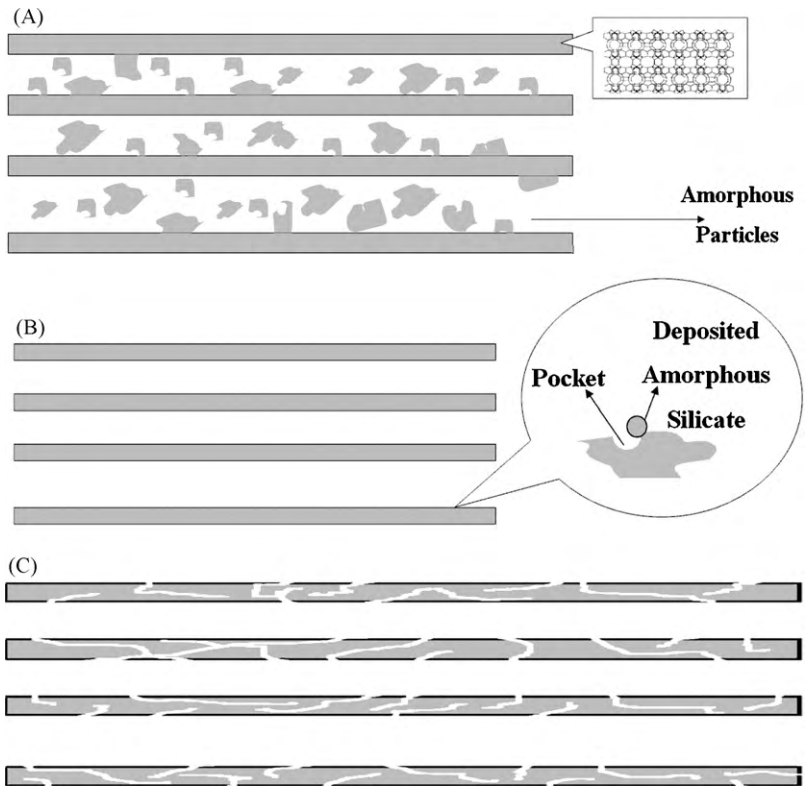

Scheme 1. Imagine of alkali-treatment process: (A) HMCM-49, (B) MCM-49 sample alkali-treated under mild conditions and (C) MCM-49 sample alkali-treated under severe conditions.

Camblor et al. reported that, when the layered precursor was transformed into the 3D framework upon calcination, most connectivity defects exist at T1–O–T1 and T2–O–T3 sites [26]. Corma et al. have succeeded in preparation of ITQ-2 with MCM-22(p) as a precursor [28], during which the potential linkages of T1–O–T1 were hindered. This indicates that T1–O–T1 linkages are more fragile than the others, and that the Si on T1 site is easily extracted with the damage of 5MR including T1 site. Fig. 2 shows that the intensities of peaks at −121 and −114.5 ppm, which are attributed to Si on $T1^+$ and T3 sites, respectively, obviously decreases compared with that of peaks of T2, T7 and T8. The peak area percent of $T1^+$ decreases from 11.52% (HMCM-49) to only 1.33% (0.65AT–75C–120M), indicating that Si atoms on T1 sites are more sensitive to alkali-treatment. Simultaneously, the percent of $Q3^+$ site increases from 8.28% (HMCM-49) to 11.22% (0.65AT–75C–120M). Thus we can conclude that Si atoms located on T1 and T3 sites are easier to be extracted than those located on other sites (T2, T7 and T8) when MCM-49 is exposed to alkali-treatment. The other Si atoms which are adjacent to T1 and T3 sites would exist in the form of $(OSi)_3SiOH$, which results in the increase of peak area centered at −98 ppm. As shown in the framework IR spectra (Fig. 3), when the NaOH solution concentration is higher than 0.2N, with the increase of NaOH solution concentration, the peaks between 540 and 630 cm^{-1} and at 1250 cm^{-1} shrink more obviously than other peaks. Especially when the NaOH solution concentration is 0.65N, the area of the peak centered at 550 cm^{-1} of 0.65AT–75C–120M shrinks to only 20% compared with that of HMCM-49, and the area of the peak at 1250 cm^{-1} also reduces by 20%. The similarity of its IR spectrum to that of ITQ-2 mentioned in Ref. [28] indicates the dissociation of T1–O–T1 linkage in 0.65AT–75C–120M. Combining with the ^{29}Si NMR results, we can propose that the extraction of Si most likely starts from the T1 and T3 sites, along with the break of blocks and damage of five member rings involving Si on T1.

The results of NH_3-TPD reveal that the total acid amount of samples alkali-treated under different conditions has a little change. The reason that 0.1AT–75C–120M possesses more strong acid sites (0.49 mmol/g) than HMCM-49 (0.44 mmol/g) can be ascribed to its higher Al content resulting from desilication. Strong acid sites of samples decrease when the concentration of NaOH is higher than 0.2N. For the sample 0.65AT–75C–120M, only 66% of strong acid sites are left compared with HMCM-49, which might be due to the collapse of zeolite framework as a result of the extraction of too much Si. Similar results are also observed on the alkali-treated ZSM-5 sample [18]. The alkali-treatment condition also has some effect on the *B*/*L* ratio of the MCM-49 samples. The *B*/*L* ratio decreases from 1.87 to 1.32 when the concentration of NaOH solution is enlarged from 0.1 to 0.65N (Table 3). The decrease of the Brønsted acid amount with the increase of alkali-treatment severity may partly account for the decrease of catalytic stability, as the Brønsted acid site of catalyst is generally considered as the active center in the reaction of ethylene alkylation with benzene [1,6]. In addition, extra mesopores are introduced (Scheme 1(C)) with the decrement of micropores (Table 2), and the catalytic stability increases at a certain degree (Fig. 6(A)) when the NaOH solution concentration is below 0.5N. This indicates that the mesopores can improve the catalytic stability by means of improving the diffusion of reactants and products [6]. The lower catalytic stability of 0.65AT–75C–120M compared with HMCM-49, is related with its low Brønsted acid amount and poor relative crystallinity, although it has a lot of mesopores.

Although the mesopore of the MCM-49 zeolite does not increase during mild alkali-treatment (c_{NaOH} = 0.025N), its total acid amount and its *B*/*L* ratio are both preserved (Fig. 5). Simultaneously, the samples alkali-treated under such conditions have limited differences in reaction performance and they all show better catalytic stability than the HMCM-49. As shown in Fig. 4, amorphous particles and crystal splinters are cleared by mild treatment with

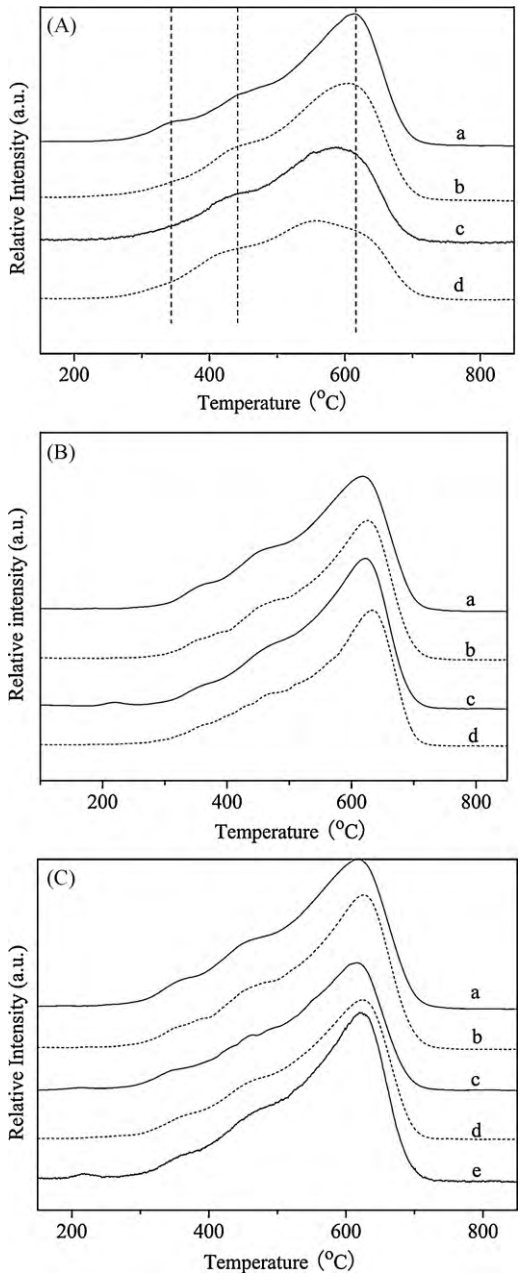

Fig. 7. TPO spectra of MCM-49 zeolites catalysts before and after alkali-treatment. (A): a: HMCM-49, b: 0.2AT–75C–120M, c: 0.5AT–75C–120M and d: 0.65AT–75C–120M; (B): a: HMCM-49, b: 0.025AT–25C–30M, c: 0.1AT–25C–30M, d: 0.1AT–75C–30M; (C): a: HMCM-49, b: 0.025AT–25C–3M, c: 0.025AT–25C–15M, d: 0.025AT–25C–30M and e: 0.025AT–25C–60M.

low NaOH concentrations such as 0.025 and 0.1N (depicted as Scheme 1(B)), during which more acid sites in the "pockets" would be exposed and it is helpful to the diffusion of reactant and product. Thus the catalytic stability is improved (Fig. 6) since the "pockets" of MWW type zeolites are the main locations for alkylation reactions [1,3]. For 0.025AT–25C–3M, its alkali-treatment time is too short to clean the amorphous particles or crystal splinters sufficiently, so it has a slightly lower stability than 0.025AT–25C–15M and 0.025AT–25C–30M. To obtain good catalytic stability for liquid alkylation of benzene with ethylene, suitable conditions of alkali-treatment for MCM-49 are as follows: 0.025N of NaOH solutions, 25 °C of treatment temperature and 15–30 min of treatment time. If the alkali-treatment time is further prolonged, a few amorphous Si species would deposit back onto the MCM-49 sheets. These small silica particles would not aggregate, but would tightly scatter on the surface [43,44], and some of the "pockets" would be partially or totally covered (marked in Scheme 1(B)). This results in the bad diffusion conditions for bigger molecular species. To some extent, this reason can account for the worse catalytic stability of 0.025AT–25C–60M being worse than that of 0.025AT–25C–15M or 0.025AT–25C–30M.

5. Conclusions

MCM-49 zeolite was alkali-treated in NaOH solution under various conditions. After the suitable alkali-treatment (in 0.025N NaOH solution at 25 °C for 15–30 min), not only are the amorphous particles and crystal splinters within the MCM-49 zeolites cleared, but also their framework and acid properties are preserved. For the severely alkali-treated samples, mesopores were introduced by the selective extraction of silicon on T1 and T3 sites in the MWW framework, covering the decrease of micropore amount as well as the damage of MCM-49 structure. In the liquid alkylation reaction of benzene with ethylene, the samples alkali-treated under mild conditions show better stability for ethylene conversion than the parent HMCM-49, and this becomes much outstanding under the high ethylene WHSV. Furthermore, the samples that were alkali-treated under severe conditions also exhibit better catalytic stability than the parent HMCM-49 unless the alkali-treatment condition is too severe.

Acknowledgement

We acknowledge the National Basic Research Program of China (Nos. 2009CB623501 and 2005CB221403) for financial support.

References

[1] A. Corma, V. Martínez-Soriab, E. Schnoevelda, J. Catal. 192 (2000) 163–173.
[2] Xinde Sun, L. Qingxia Wang, S. Xu, Liu, Catal. Lett. 94 (2004) 75–79.
[3] J.C. Cheng, T.F. Degnan, J.S. Beck, Y.Y. Huang, M. Kalyanaraman, J.A. Kowalski, C.A. Loehr, D.N. Mazzone, Stud. Surf. Sci. Catal. 121 (1999) 53–60.
[4] C. Perego, P. Ingallina, Catal. Today 73 (2002) 3–22.
[5] J.C. Groen, L. Peffer, J. Moulijn, J. Pérez-Ramírez, Chem. Eur. J. 11 (2005) 4983–4994.
[6] G. Bellussi, G. Pazzuconi, C. Perego, G. Girotti, G. Terzoni, J. Catal. 157 (1995) 227–234.
[7] S. Lawton, A. Fung, G. Kennedy, L. Alemany, C. Chang, G. Hatzikos, D. Lissy, M. Rubin, H. Timken, S. Steuernagel, J. Phys. Chem. 100 (1996) 3788–3798.
[8] J.M. Bennett, C.D. Chang, S.L. Lawton, M.E. Leonowicz, D.N. Lissy, M.K. Rubin, B. Cynwyd, US Patent 5236575, 1993.
[9] G. Kennedy, S. Lawton, A. Fung, M. Rubin, S. Steuernagel, Catal. Today 49 (1999) 385–399.
[10] J. Cheng, C. Smith, D. Walsh, US Patent 5493065, 1996.
[11] Y. Tao, H. Kanoh, L. Abrams, K. Kaneko, Chem. Rev. 106 (2006) 896–910.
[12] A.H. Janssen, A.J. Koster, K.P.d. Jong, Angew. Chem. Int. Ed. 40 (2001) 1102–1104.
[13] R. Giudici, H.W. Kouwenhoven, R. Prins, Appl. Catal. A: Gen. 203 (2000) 101–110.
[14] R. Dutartre, L.C. de Meorval, F. Di Renzo, D. McQueen, F. Fajula, P. Schulz, Micropor. Mater. 6 (1996) 311–320.
[15] J.C. Groen, L.A.A. Peffer, J.A. Moulijn, J. Pérez-Ramírez, Micropor. Mesopor. Mater. 69 (2004) 29–34.
[16] J.C. Groen, J.A. Moulijn, J. Pérez-Ramírez, J. Mater. Chem. 16 (2006) 2121–2131.
[17] Y. Tao, H. Kanoh, K. Kaneko, Adsorption 12 (2006) 309–316.
[18] Y. Li, S. Liu, Z. Zhang, S. Xie, X. Zhu, L. Xu, Appl. Catal. A: Gen. 338 (2008) 100–113.
[19] D.A. Young, Y. Linda, US Patent 3326797, 1967.
[20] G.T. Kokotailo, A.C. Rohrman, US Patent 4703025, 1987.
[21] L. Mokrzycki, B. Sulikowski, Z. Olejniczak, Catal. Lett. 127 (2009) 296–303.
[22] G.T. Kokotailo, C.A. Fyfe, The Regaku J. 12 (1995) 3–10.
[23] C.A. Emeis, J. Catal. 141 (1993) 347–354.
[24] X. Wei, P.G. Smirniotis, Micropor. Mesopor. Mater. 97 (2006) 97–106.
[25] C. Delitala, M.D. Alba, A.I. Becerro, D. Delpiano, D. Meloni, E. Musu, I. Ferino, Micropor. Mesopor. Mater. 118 (2009) 1–10.
[26] M.A. Camblor, C. Corell, A. Corma, M.-J. Diaz-Cabanas, S. Nicolopoulos, J.M. Gonzalez-Calbet, M. Vallet-Regi, Chem. Mater. 8 (1996) 2415–2417.
[27] A.v. Miltenburg, J. Pawlesa, A.M. Bouzga, N. Žilková, J. Čejka, M. Stöcker, Top. Catal. 52 (2009) 1190–1202.
[28] A. Corma, V. Fornes, S.B. Pergher, T.L.M. Maesen, J.G. Buglass, Nature 396 (1998) 353–356.

[29] A. Corma, C. Corell, V. Fornés, W. Kolodziejski, J. Pérez-Pariente, Zeolites 15 (1995) 576–582.
[30] A. Corma, C. Corell, J. Pérez-Pariente, J.M. Guil, R. Guil-López, S. Nicolopoulos, J.G. Calbet, M. Vallet-Regi, Zeolites 16 (1996) 7–14.
[31] A. Corma, C. Corell, J. Pérez-Pariente, Zeolites 15 (1995) 2–8.
[32] G. Xu, X. Zhu, X. Niu, S. Liu, S. Xie, X. Li, L. Xu, Micropor. Mesopor. Mater. 118 (2009) 44–51.
[33] J. Pawlesa, M. Bejblová, L. Sommer, A.M. Bouzga, M. Stöcker, J. Čejka, Stud. Surf. Sci. Catal. 170 (2007) A610–A615.
[34] J.C. Groen, L.A.A. Peffer, J.A. Moulijn, J. Pérez-Ramíez, Colloid Surf. A 241 (2004) 53–58.
[35] X. Li, R. Prins, J.A. van Bokhoven, J. Catal. 262 (2009) 257–265.
[36] A. Bonilla, D. Baudouin, P.-R. Javier, J. Catal. 265 (2009) 170–180.
[37] L.L. Su, L. Liu, J.Q. Zhang, H.X. Wang, Y.G. Li, W.J. Shen, Y.D. Xu, X.H. Bao, Catal. Lett. 91 (2003) 155–167.
[38] L.L. Su, Y.G. Li, W.J. Shen, Y.D. Xu, X.H. Bao, Stud. Surf. Sci. Catal. 147 (2004) 595–600.
[39] M. Ogura, S. Shinomiya, J. Tateno, Y. Nara, E. Kikuchi, M. Matsukata, Chem. Lett. 29 (2000) 882–883.
[40] T. Suzuki, T. Okuhara, Micropor. Mesopor. Mater. 43 (2001) 83–89.
[41] J.C. Groen, J.C. Jansen, J.A. Moulijn, J. Pérez-Ramírez, J. Phys. Chem. B 108 (2004) 13062–13065.
[42] M. Ogura, S. Shinomiya, J. Tateno, Y. Nara, M. Nomura, E. Kikuchi, M. Matsukata, Appl. Catal. A: Gen. 219 (2001) 33–43.
[43] A. Cizmek, B. Subotic, R. Aiello, F. Crea, A. Nastro, C. Tuoto, Micropor. Mater. 4 (1995) 159–168.
[44] A. Cizmek, B. Subotic, I. Smit, A. Tonejc, R. Aiello, F. Crea, A. Nastro, Micropor. Mater. 8 (1997) 159–169.